

Cell permeable Imidazole-Desferrioxamine Conjugates: Synthesis and in-vitro Evaluation

Shreya Pramanik, Saikat Chakraborty, Malavika Sivan, Birija Patro, Sucheta Chatterjee, and Dibakar Goswami

Bioconjugate Chem., **Just Accepted Manuscript** • DOI: 10.1021/acs.bioconjchem.8b00924 • Publication Date (Web): 14 Feb 2019

Downloaded from <http://pubs.acs.org> on February 17, 2019

Just Accepted

“Just Accepted” manuscripts have been peer-reviewed and accepted for publication. They are posted online prior to technical editing, formatting for publication and author proofing. The American Chemical Society provides “Just Accepted” as a service to the research community to expedite the dissemination of scientific material as soon as possible after acceptance. “Just Accepted” manuscripts appear in full in PDF format accompanied by an HTML abstract. “Just Accepted” manuscripts have been fully peer reviewed, but should not be considered the official version of record. They are citable by the Digital Object Identifier (DOI®). “Just Accepted” is an optional service offered to authors. Therefore, the “Just Accepted” Web site may not include all articles that will be published in the journal. After a manuscript is technically edited and formatted, it will be removed from the “Just Accepted” Web site and published as an ASAP article. Note that technical editing may introduce minor changes to the manuscript text and/or graphics which could affect content, and all legal disclaimers and ethical guidelines that apply to the journal pertain. ACS cannot be held responsible for errors or consequences arising from the use of information contained in these “Just Accepted” manuscripts.

Cell permeable Imidazole-Desferrioxamine Conjugates: Synthesis and in-vitro Evaluation

Shreya Pramanik,^{a,+} Saikat Chakraborty,^{b,+} Malavika Sivan,^{c,+} Birija S Patro,^{b,d} Sucheta Chatterjee,^b and Dibakar Goswami^{b,d*}

^aCentre for excellence in Basic Sciences, Mumbai, PIN: 400098, India

^bBio-Organic Division, Bhabha Atomic Research Centre, Trombay, Mumbai, PIN: 400085, India

^cIISER, Bhopal, PIN: 462066, India,

^dHomi Bhabha National Institute, Anushaktinagar, Mumbai, PIN: 400094, India

⁺Equal contributions

^{*}Corresponding author

ABSTRACT.

Desferrioxamine (DFO), a clinically approved iron chelator used for iron overload, is unable to chelate labile plasma iron (LPI) due to its limited cell permeability. Herein, alkyl chain modified imidazolium cations with varied hydrophobicities have been conjugated with DFO. The iron binding abilities, and the antioxidant properties of the conjugates were found to be similar to DFO. The degree of cellular internalisation was much higher in the octyl-imidazolium-DFO conjugate (**IV**) compared to DFO, and was able to chelate LPI in-vitro. This opens up a new avenue in using *N*-alkyl imidazolium salts as a delivery vector for hydrophilic cell-impermeable drugs.

KEYWORDS. *N*-alkyl imidazolium salts; Desferrioxamine; hydrophobicity; Chelation; Labile plasma iron.

Introduction

Iron is the most abundant metal on earth, and is a vital constituent of human body.¹ It plays important roles in oxygen transport, DNA synthesis and in the formation of several biologically important enzymes. However, due to the redox toxicity of the labile iron, its absorption, distribution, utilization and storage in human body is tightly regulated.^{2,3} At the same time, there are certain conditions (e.g. hereditary hemochromatosis, β -thalassemia etc.) which lead to excess iron accumulation in human body. These iron pools, either accumulated in plasma (labile plasma iron, LPI) or in cytosol (labile iron pool, LIP), generates reactive oxygen species (ROS) *via* Fenton/Heber-Weiss reactions, thereby promoting oxidative stress leading to cell death *via* lipid peroxidation and/or DNA damage.⁴

Chelation therapy, used for the treatment of iron overload and to maintain a steady and healthy iron concentration in human body, has gained considerable attention in the last few years.⁵ Three chelators viz. desferrioxamine B (DFO), deferiprone (DFP) and deferisirox (DFX) are being regularly used in clinical practice. Apart from these, a large number of other chelators have also been developed and are under different phases of trial.⁶ Amongst these, DFO, a highly specific hydroxamate based iron chelator, has been used for last 50 years with a high success rate.⁷ However, its poor gastrointestinal absorptivity, and subsequent poor bioavailability renders this drug to be administered as a parental infusion, leading to poor patient compatibility.⁸ DFP, despite its better bioavailability and promising results when used in combination with DFO or DFX, has limited clinical use due to some serious side-effects.^{9,10} Moreover, both bidentate (DFP) and tridentate (DFX) ligands can form partially chelated complexes, and may be susceptible for redox recycling, which is detrimental and undesirable.¹¹ DFO, which forms strong hexa-coordinate complex with iron, is the most advantageous and the most preferred chelator for clinical uses.

However, the limiting cell-permeability of DFO, mainly due to its high hydrophilicity coupled with high molecular weight, has restricted its use for chelation of LIP. The “free”

LIP in the Fe-loaded cells has significant toxicity, and hence is an important and invincible target for iron chelators.¹² To overcome this limitation, a number of DFO-conjugates e.g. with lipophilic adamantyl groups,¹³ caffeine,¹⁴ peptides,^{4,15,16} triphenylphosphonium,¹⁷ different lipophilic antioxidants¹⁸ etc. have been synthesized and evaluated for membrane permeability. However, none of these conjugates have been approved as a chelator for clinical use, and hence, search for an “ideal” conjugate continues.

Recently, imidazolium based compounds have shown increased antimicrobial activities.¹⁹ Similar kinds of salts are also being considered as a potential tool for delivering active pharmaceutical ingredients (API) across cells.²⁰ The API can be linked to the cationic imidazolium core either as an anion²¹ or *via* covalent bonding.²⁰ Their properties, specially hydrophilicities of the conjugates, can be tailored using different substituents, and hence this offers a major advantage of using imidazolium salts as delivery vectors. In this study, we have conjugated DFO with imidazolium cations having varied alkyl substituents, thereby possessing different degrees of hydrophobicity (**Fig. 1**, compounds **I-IV**). These conjugates were evaluated for their iron binding abilities, their antioxidant properties, and their cell permeability, compared to the parent siderophore.

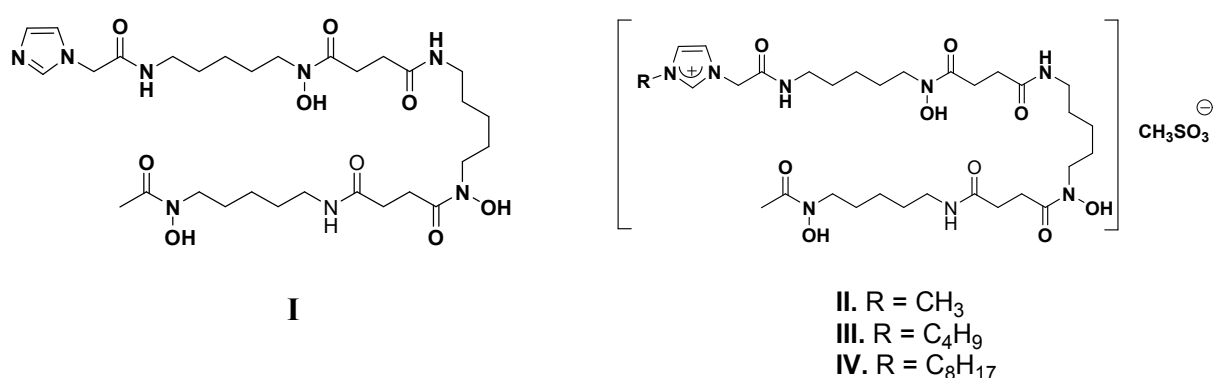
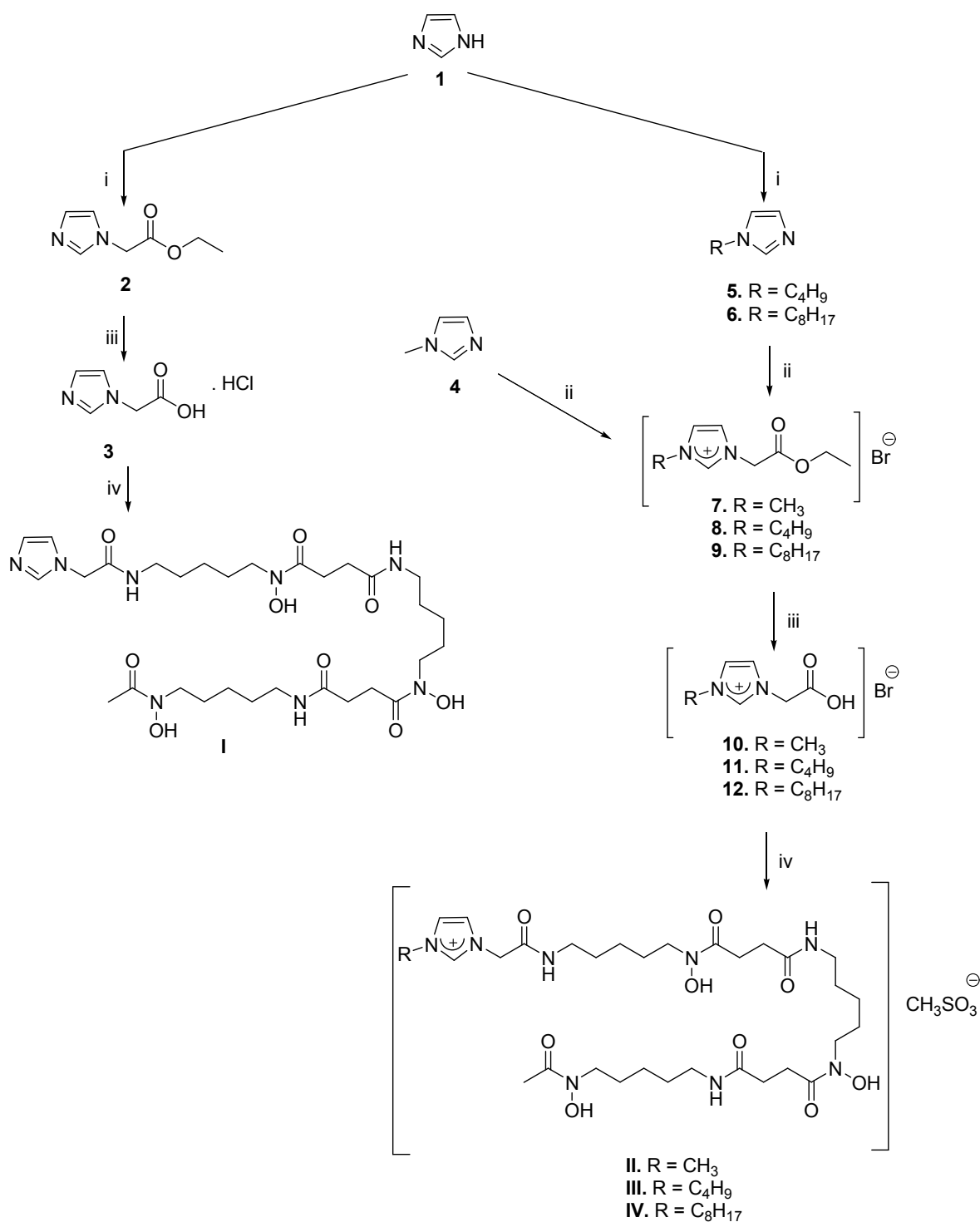


Fig. 1. Structures of imidazole-DFO conjugates (**I-IV**).

Results

Synthesis of imidazole-desferrioxamine conjugates I-IV

Imidazole-DFO conjugates (**I-IV**) were prepared according to **Scheme 1**. For synthesis of conjugate **I**, imidazole (**1**) was reacted with ethyl bromoacetate, followed by acid hydrolysis and subsequent conjugation to DFO using reported procedure.^{22,23} For conjugate **II**, commercially available *N*-methyl imidazole (**4**) was similarly reacted with ethyl bromoacetate, followed by acid hydrolysis and subsequent conjugation to DFO. Conjugates **III** and **IV** were synthesized similarly using *N*-butyl imidazole (**5**) and *N*-octyl imidazole (**6**) respectively.



Scheme 1. Synthesis of conjugates **I-IV**.

Purification and characterization

The crude conjugates **I-IV** were purified by semi preparative RP-HPLC using Younglin RP-HPLC semi preparative system Model YL9100 consisting of a quaternary pump (YL9110S), an UV detector (YL9120 Dual Absorbance Detector), a manual sample injector, an automated gradient controller and a semi-preparative column (Venusil XBP C 18), at a flow rate of 2.0 mL/min (solvent A: 0.1% TFA/water and solvent B: 60% AcCN/0.1% TFA). The absorbances were monitored at a wavelength of 254 nm, and the gradient applied was 5% B to 95% B in 90 min.

After purification, the analysis of the purified conjugates **I-IV** was performed in a Younglin HPLC system (analytical column Kromasil® C18) with a flow rate of 1.0 mL/min using the same solvents and gradient as mentioned above. The absorbance was monitored at a wavelength of 254 nm. All the conjugates were characterized by ¹H NMR (using Bruker AC-200 instrument or 500 MHz Varian NMR spectrometer, as described before and also in *SI*), CHN-analysis (using Elementar Vario micro cube), and FT-IR (as pellets in KBr, using a BRUKER Tensor II spectrophotometer) spectroscopy. The retention times (*R_t*) in analytical RP-HPLC and the calculated and experimental results of CHN analyses of the purified conjugates are tabulated in Table 1.

Table 1. Results of analytical RP-HPLC and elemental analysis for conjugates **I-IV**.

Conjugate	RP-HPLC		Elemental Analysis							
	<i>R_t</i> (min)	Purity (%)	Calculated (%)				Experimental (%)			
			C	H	N	S	C	H	N	S
I	23.8	97.8	53.88	7.84	16.75	-----	53.64	7.68	16.98	-----
II	20.2	95.6	49.34	7.51	14.39	4.12	49.06	7.48	14.75	3.74
III	12.8	91.1	51.20	7.86	13.65	3.91	50.81	7.74	13.96	4.17
IV	16.5	93.6	53.41	8.27	12.78	3.66	53.12	8.62	12.95	3.64

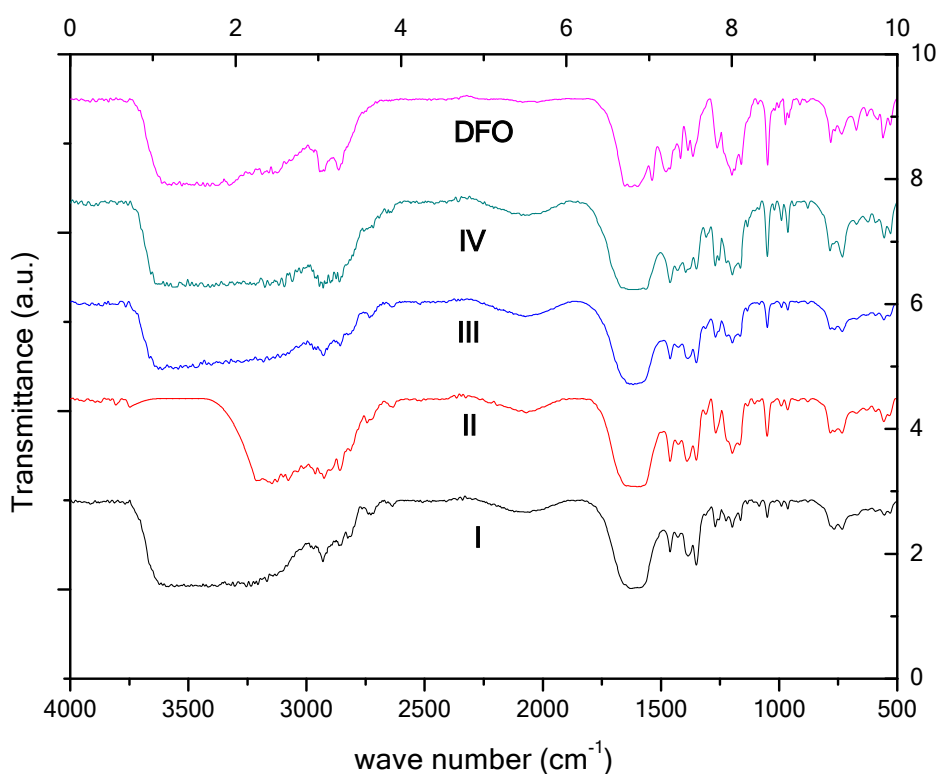


Fig. 2. FT-IR spectra of DFO and conjugates **I-IV**.

Table 2. Selected FT-IR peaks obtained in conjugates **I-IV** vis-à-vis DFO

Vibration mode	DFO (cm ⁻¹)	I (cm ⁻¹)	II (cm ⁻¹)	III (cm ⁻¹)	IV (cm ⁻¹)
-N-OH	1640	1638	1648	1627	1641
-N-H stretching	3480	3491	3203	3487	3486
-CH ₂ stretching	2936 (asymmetric)	2938	2921	2931	2935
	2859 (symmetric)	2854	2855	2859	2859
CO stretching	1627	1627	1634	1627	1620
-CH ₂ bending	1474	1464	1460	1463	1464
C-C stretching	1162	1162	1166	1159	1165
N-O stretching	1048	1050	1049	1051	1049
Imidazolium N-C-N stretching	absent	1567	1567	1570	1562

FT-IR spectra of the conjugates were recorded in KBr pellets, and compared with DFO (Fig. 2). It could be observed that hydroxamic group vibration ($\sim 1640\text{ cm}^{-1}$)²⁴ appear in the spectra of DFO alongwith all the compounds **I-IV**, indicating the presence of unaffected chelator moiety in the conjugates. Although the -C=C- stretching vibration of the imidazolium ring ($\sim 1640\text{ cm}^{-1}$)²⁵ was masked (due to overlapping N-OH vibration) in the spectra of the conjugates **I-IV**, the conjugation of imidazolium group to DFO could be ascertained from the presence of imidazolium N-C-N stretching mode ($\sim 1565\text{ cm}^{-1}$) in the spectra of **I-IV**.^{26,27} The other vibrations,²⁸ typically suggesting the unaltered chelating moiety in the conjugates are tabulated in **Table 2**.

Table 3. Calculated $\log P_{ow}$ values for DFO-mesylate and conjugates **I-IV**

Compound	DFO-Mes	I	II	III	IV
$\log P_{ow}$	-6.39	-3.41	-6.82	-5.61	-4.03

The calculated (using MarvinSketch software²⁹) $\log P_{ow}$ (octanol/water) values for DFO-Mes (neutral form, ammonium cation with methane sulphonate as counter anion and conjugates **I-IV** (neutral form for conjugate **I**; neutral forms for DFO and conjugates **II-IV** with either ammonium or imidazolium cation and methane sulphonate as counter anion, no micro species with gross charges were taken into account) are tabulated in **Table 3**. Conjugates **II** and **III** were calculated to be highly hydrophilic, almost comparable to DFO. Conjugates **I** and **IV** were comparatively hydrophobic, showing promise for better cellular uptake. Experimentally, the solubility of conjugates **II** and **III** in water (pH 7.4, $> 3\text{ mg/mL}$) was much higher than those of conjugates **I** and **IV** ($< 1\text{ mg/mL}$). This corroborates with the calculated $\log P_{ow}$ values. Stock solutions of **II** and **III** in HBS, and **I** and **IV** in DMSO were prepared. Unless otherwise mentioned, the DMSO solutions were properly diluted in HBS for further experiments.

Iron binding studies

The iron-binding of conjugates **I-IV** was checked by UV electronic spectroscopy (Fig. 3), and was compared with that of desferrioxamine (DFO). All the spectra were collected with 10% aqueous DMSO solutions. Addition of ferrous ammonium sulfate (FAS) to DFO or DFO-conjugates **I-IV** invariably formed Fe(III) complexes of the chelators, via the rapid autooxidation of Fe(II) to Fe(III).^{30,31} All the solutions showed absorbance maxima around 430 nm, which is typical signature of formation of ferrioxamine complex, thus indicating that the chelator moiety was preserved in the conjugates.

The stoichiometry of iron-binding to compounds **I-IV** were assessed by continuous variation (Job's) method^{14,32} and compared to the parent DFO molecule. The solutions of FAS, DFO and compound **I-IV** were all prepared in 10% aqueous DMSO. After addition of instantly prepared FAS solution to the solutions of DFO and compounds **I-IV**, the solutions were mixed properly, and were equilibrated for approx. 30 min. The UV-VIS spectra of the solutions were recorded at 28 °C. In this method total concentration of added iron and compound **I-IV** were kept constant, and their relative proportions, i.e. mole fractions (X_i), were varied. Change in absorbance of the complex at 430 nm (or in principle any parameter which varies linearly with concentration), when plotted against the mole fraction of either metal or ligand, is expected to show curvature plot with maxima at $X_L = 0.5$ for complexation with 1:1 stoichiometry (*cf.* Fig. 4). Moreover, the shape of the curve provides qualitative insight into binding equilibrium ($K_{eq} = [ML]/([M][L])$); where strong binding results $K_{eq} \gg 1$ and curvature approaches a perfect triangle, as observed for all the four compounds. The data were analysed according to the procedures reported by Renny et al.³³ The stoichiometry of iron binding to all the conjugates (**I-IV**) and DFO were virtually identical (Fig. 4) and equal to 1:1 (metal:ligand) stoichiometry. Again, the imidazole conjugation to DFO did not alter iron binding equilibrium significantly and did not add extra binding sites.

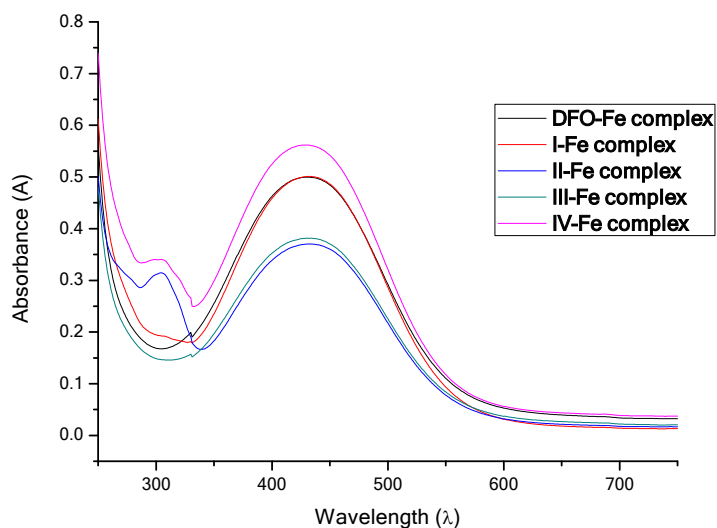


Fig. 3. UV-VIS spectra of iron complexes of DFO and conjugates I-IV (50 μ M solutions of Fe-chelator prepared in 10% DMSO were used in each case).

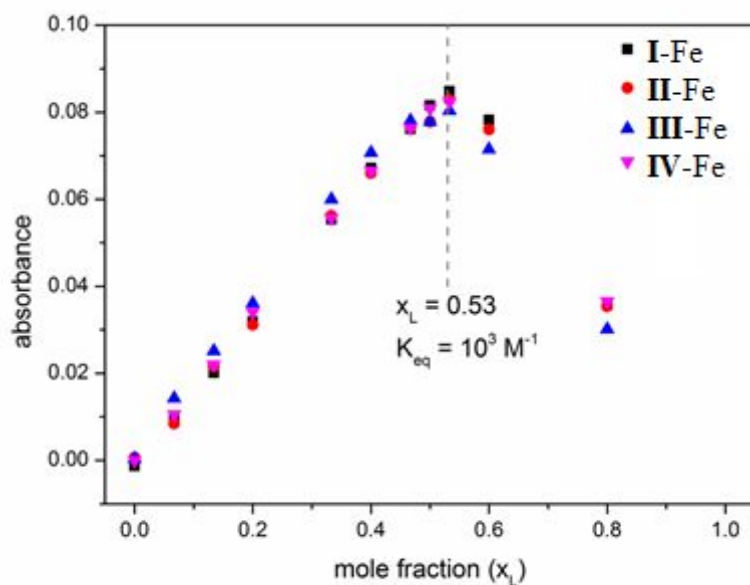


Fig. 4. Job's plots for the binding of iron to conjugates I-IV (absorbance recorded at 430 nm).

Competition studies with calcein³⁴

Calcein, a well-known metal-sensor, shows stoichiometric quenching of its fluorescence in presence of iron(III).³⁵ This property has been extensively used for determining labile iron concentration in biological fluids. In presence of a stronger iron chelator, the calcein-iron (Ca-Fe) complex may get disrupted, and the calcein fluorescence is recovered. Since the fluorescence quenching of calcein is faster in presence of iron (II),³⁶ competition studies with the proposed chelators have been conducted using aqueous Fe(II) solution. Rapid autoxidation of Fe(II) to Fe(III) happens upon binding to calcein in ambient air. At physiological pH, addition of different chelators (with higher Fe(III) binding affinity) to the solution of Ca-Fe(III) led to fluorescence recovery (Fig. 5), the extent of which is dependent on the relative affinities of the iron chelators. As evident from Fig. 5, all the chelators efficiently competed with calcein, and their iron-binding profiles were similar to that of DFO. This indicated the high thermodynamic stability of the iron-complexes of the proposed chelators, indicating their possible roles in physiological iron scavenging. The profile also indicated that the iron binding ability of the DFO was retained in their imidazole-conjugates.

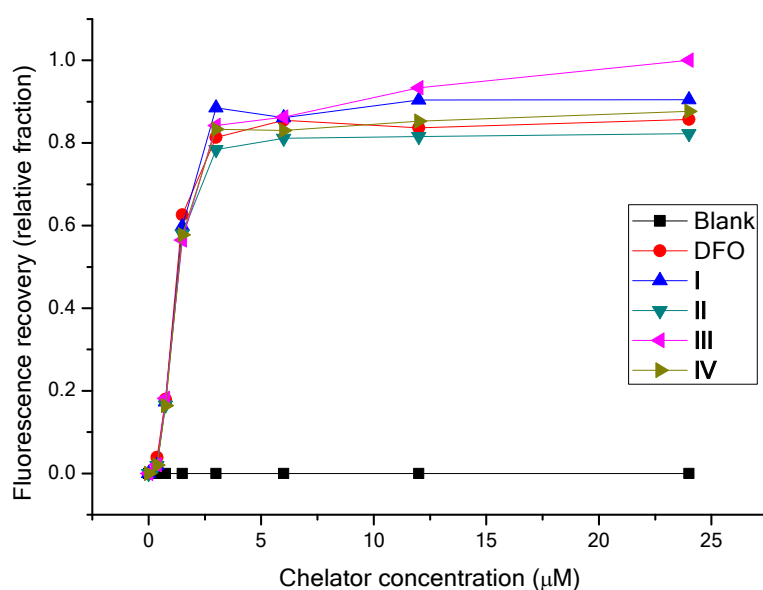
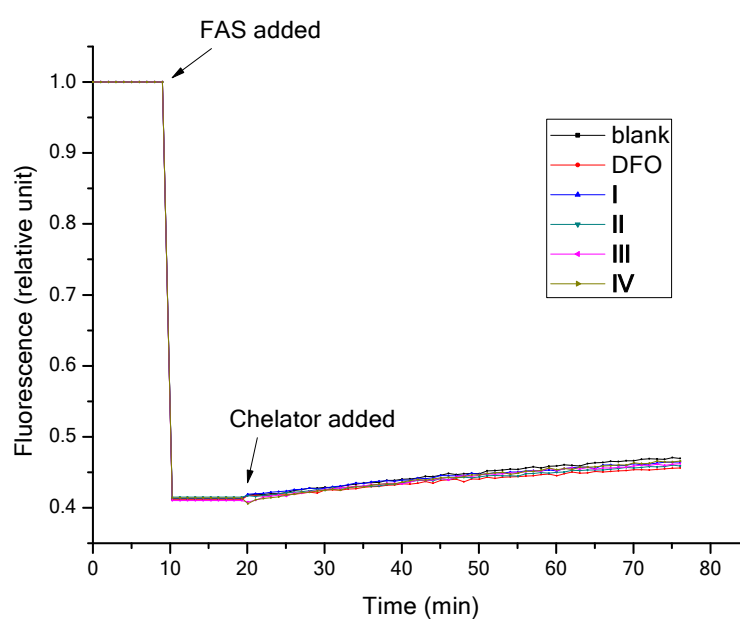


Fig. 5. Dequenching of calcein (2 μM) fluorescence as a function of chelator concentration
(The plot represents the average of duplicate experiments repeated at least twice).

Competition studies with fluorescein-apotransferrin

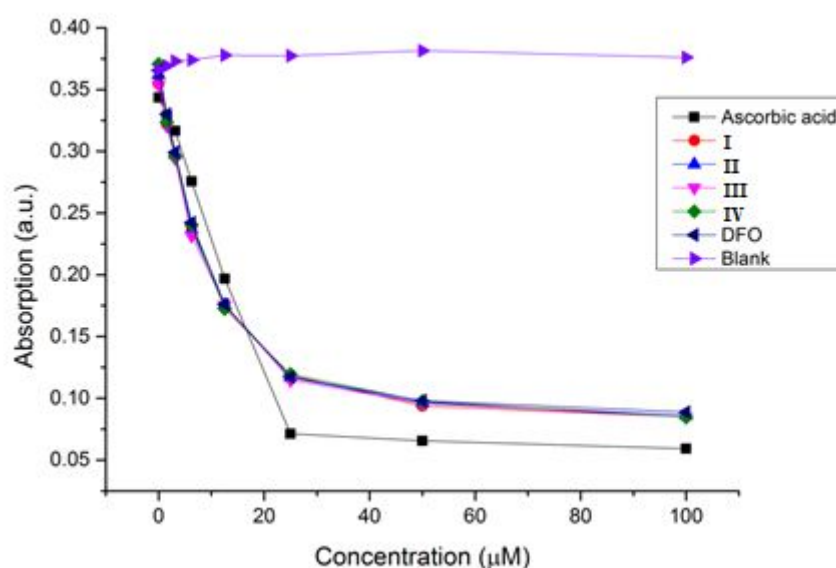
Fluorescein-labeled apotransferrin (Fl-aTf) was first used by Bruer and Cabantchik for the assay of non-transferrin-bound iron (NTBI).³⁷ Following the reported procedure,³⁷ Fl-aTf was prepared by incubating 5-DTAF with holo-transferrin, and subsequent dialysis against citrate (pH 5.5). This Fl-aTf undergoes fluorescence quenching upon binding iron, and this property has been used for assessing the ability of the proposed chelators to remove iron from the diferric transferrin. DFO, despite its higher affinity towards iron, cannot remove iron from transferrin, mainly due to kinetic reasons. The same is also true for the proposed chelators. The chelators, even at a 2-fold concentration of the Fl-Tf-Fe₂, was not able to demetallise it (Fig. 6). This, in turn, is an important positive characteristic of the chelators since these should not remove excess iron affecting its biochemical compartments.



1 **Fig. 6.** Recovery of fluorescence from aqueous FI-Tf-Fe₂ solution (2 μM) by addition of 20
2 μM of chelators (The plot represents the average of duplicate experiments repeated at least
3 twice).
4
5
6
7
8
9
10
11
12

13 *DPPH assay*

14
15 DPPH (2,2-diphenyl-1-picrylhydrazyl) is a stable free radical at room temperature, and
16 gives a violet colour when dissolved in methanol. However, in presence of an antioxidant, the
17 radical is scavenged, and the colour is discharged. This is used to assay the antioxidant
18 property of a compound spectrophotometrically.³⁸ All the chelators under study, along with
19 the standard antioxidant ascorbic acid, decreased the amount of DPPH in the solution (Fig.
20 7). This invariably established the antioxidant properties of the chelators.
21
22
23
24
25
26
27
28
29



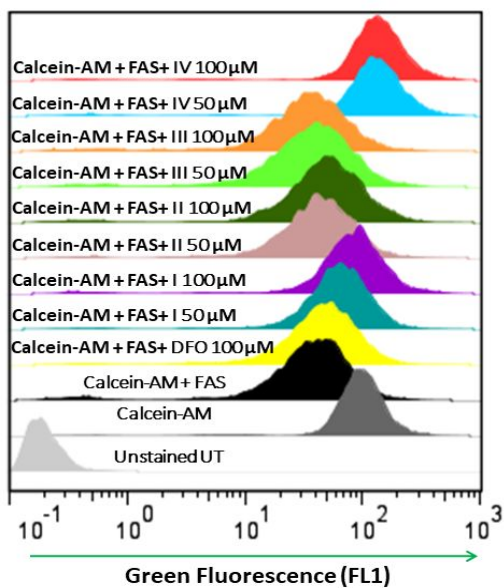
30
31
32
33
34
35
36
37
38
39
40
41
42
43
44
45
46
47
48 **Fig. 7.** DPPH radical scavenging activity of conjugates I-IV compared to DFO and ascorbic
49 acid (The plot represents the average of duplicate experiments repeated at least twice).
50
51
52
53
54
55

56 *Chelation of cellular LIP*

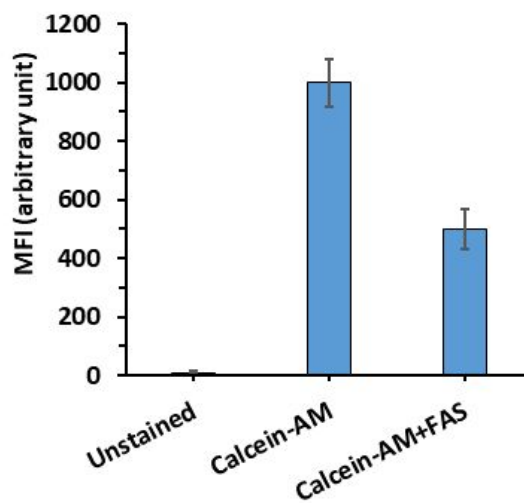
57
58 In order to assess cell permeability and chelation of intracellular LIP by compound I-
59 IV, a flow cytometry based fluorescence analysis of calcein acetoxymethyl ester (calcein-
60

1 AM), a cell permeable iron sensor, was adopted.³⁹ To this end, U2-OS (osteosarcoma) cells
2
3 were used as a cellular model. In this assay, cellular esterases hydrolyses calcein-AM to
4
5 calcein, which is fluorescent. Calcein fluorescence is quenched upon its binding to cellular
6
7 LIP, in a stoichiometric fashion.³⁹ In accordance to previous report, our result showed that the
8
9 mean fluorescence intensity (MFI), which was ~0.1 in unstained cells, increased to ~100 in
10
11 CA-AM loaded cells (Fig. 8A, B). Upon FAS treatment, which enhances LIP, calcein
12
13 fluorescence was significantly reduced in the cells. This result confirmed the specificity of
14
15 the assay for measuring LIP. Addition of iron chelator, which removes iron from its complex
16
17 with calcein, increases the fluorescence emitted by the cells.³⁹ The difference in the cellular
18
19 MFI (ΔF) with and without iron chelator incubation depicts the cell permeation and LIP
20
21 chelating properties of chelators.⁴⁰ In our experiment, DFO (100 μM) caused only marginal
22
23 increase in ΔF . As shown in Fig. 8A, C, compound **II-III** (50 and 100 μM) has no or marginal
24
25 effect on ΔF . Interestingly, compound **I** and **IV** enhanced ΔF significantly, in a concentration
26
27 dependent manner. The LIP chelation efficiency of **IV** was higher in comparison to **I**.
28
29 Together, this result suggested that compound **I** and **IV**, especially **IV**, dequenched calcein
30
31 fluorescence most effectively by efficient penetration and chelating LIP in the cells, whereas
32
33 DFO and compound **II**, **III** did not have a significant effect on ΔF , due to their poor cell
34
35 permeating abilities. Moreover, a similar result was also observed in MCF7 (breast
36
37 carcinoma) cells (data not shown). Together, our result suggested that the LIP chelation
38
39 efficiency of **IV** is not limited to one cell type.
40
41
42
43
44
45
46
47
48
49
50
51
52
53
54
55
56
57
58
59
60

A



B



C

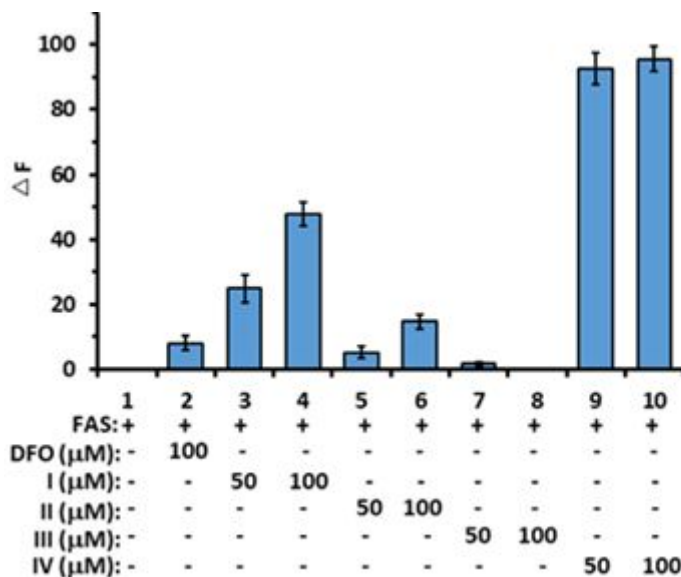


Fig. 8. Flow cytometry measurements of LIP and its chelation by compound I-IV. U2-OS cells were loaded with 0.2µM calcein-AM for 30 min, then washed and treated with FAS (50

1 μM) and ascorbic acid (200 μM), for 30 min, to enhance the cellular LIP. Subsequently, cells
2
3
4 were washed and treated the iron chelators (50 and 100 μM) for 60 min and acquired by flow
5
6 cytometry. (A-C) Mean fluorescence intensities (MFI) in histograms of unstained cells (no
7
8 calcein-AM), calcein-stained cells under different treatment were quantified by FlowJo
9
10 software. The difference in the MFI in absence and presence of chelator represents ΔF , which
11
12 was used as a measure of LIP.
13
14

15 16 17 18 *Cytotoxicity and cellular uptake assay*

19
20 Higher LIP chelation efficiency of compound **I** and **IV** indicated a better cellular
21
22 permeability and intracellular availability of compound **I** and **IV**, as compared to DFO.
23
24 However, higher cellular permeability of these conjugates may leads to higher cytotoxicity.
25
26 In order to assess compound **I-IV** and DFO induced cytotoxicity, U2-OS cells were treated
27
28 with these compounds (200 μM) and cell viability was measured at 24-72 h by MTT assay.
29
30 Our results showed that compound **I-IV** induces no or marginal loss of cell viability during
31
32 24-72 h treatment (Fig. 9A).
33
34

35
36 In order to assess the mode of cellular uptake, the LIP chelating ability of compound
37
38 **IV** was assessed in the absence and presence of sucrose (inhibits clathrin mediated
39
40 endocytosis), nystatin (inhibits caveolae mediated endocytosis) and nocodazole (inhibits
41
42 macropinocytosis).⁴¹ Cellular uptake of compound **IV** was chosen for further study because
43
44 of its superior LIP chelating efficiency *vis-à-vis* other tested compounds in the current study.
45
46 To this end, our results showed that pre-incubation of cells with sucrose, nystatin or
47
48 nocodazole partially but significantly reduces compound **IV** mediated chelation of LIP in
49
50 cells (Fig. 9B). In control experiment, sucrose, nystatin or nocodazole treatment alone has no
51
52 or marginal effects on LIP status in the cells. Together, this suggested that cellular uptake of
53
54 compound **IV** is mediated through multiple processes *via* endocytosis and macropinocytosis.
55
56
57
58
59
60

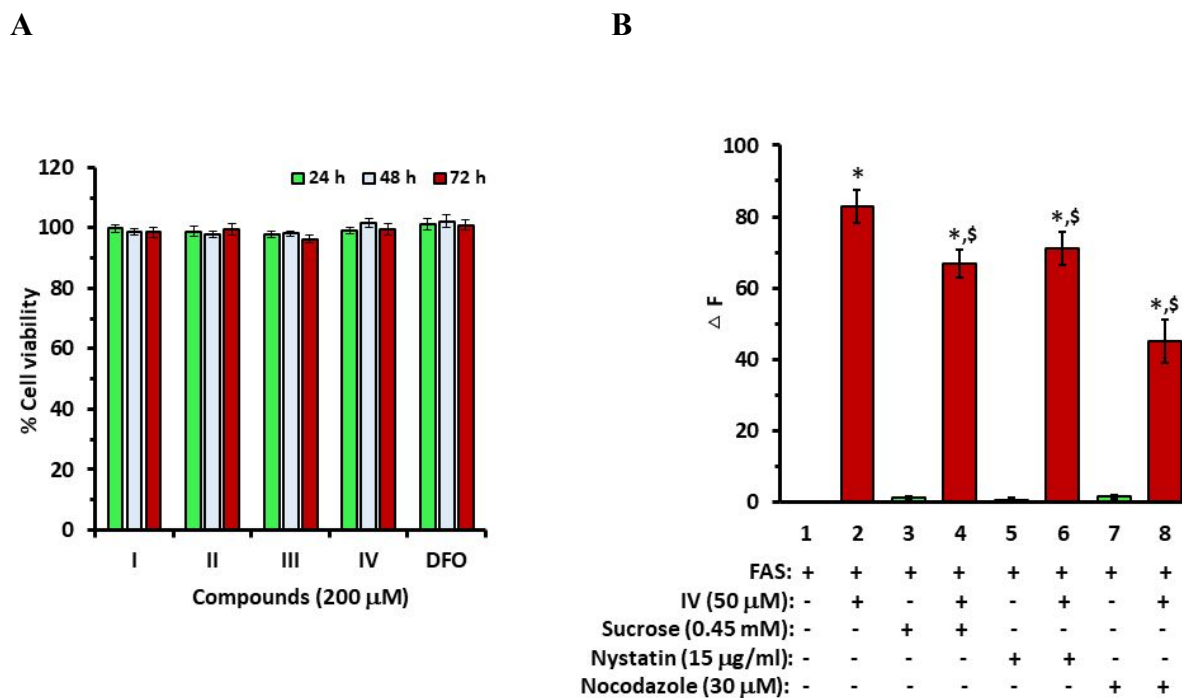


Fig. 9. Cytotoxic and cellular uptake analysis. **(A)** U2-OS cells were treated with compound **I-IV** or DFO (200 μM) for 24-72 h. Cells viability was assessed by MTT assay. **(B)** U2-OS cells were loaded with calcein-AM (0.2 μM) for 30 min, then washed and treated with FAS (50 μM) and ascorbic acid (200 μM), for 30 min, to enhance the cellular LIP. Further cells were washed and incubated with medium containing either sucrose, nystatin or nocodazole for 60 min. Subsequently, compound **IV** (50 μM) was added for 60 min and cellular fluorescence was acquired by flow cytometry. The difference in the MFI in absence and presence of chelator represents ΔF , which was used as a measure of LIP. The experiments were repeated three times. All determinations were made in 2-3 replicates and the values are mean \pm S. E. M. * $p < 0.05$ compared to respective control in the absence of compound **IV**, \$ $p < 0.05$ compared to FAS + compound **IV**.

Discussion

Iron overload is inevitable in many diseases including hemochromatosis, thalassemia, myelodysplastic syndromes etc., where excess iron accumulation can occur via increased gastrointestinal absorption or *via* transfusional loading. This excess iron, both extracellular (NTBI, non-transferrin bound iron) and intracellular (LIP) can be detrimental to human health. Very recently, LIP level has been suggested as an alternative marker for iron overload and related oxidative stress in β -thalassemia patients.⁴² This, unambiguously, shows the importance of LIP as a target in chelation therapy. Although DFX and DFP, either used separately or in combination with DFO, have showed considerable improvements in LIP removal, their potential toxicity has always been a concern. Towards this, derivatives of DFO with increased cell permeability, and unaffected chelation ability can be used as suitable alternatives.

Earlier, imidazolium salts have been shown to possess antimicrobial properties.^{19,43} Their cell permeability increases with increasing alkyl chain length, as shown in Hep-G2 cells.⁴⁴ This property of imidazolium salts has been utilised for delivering APIs across cells,^{20,21} as well as delivery reagent for siRNA.⁴⁵ However, imidazolium salts have never been used for delivering metal chelators across cells.

In this study, in a first ever attempt, we have conjugated imidazolium salts with DFO. The synthetic strategy enabled us to tailor the hydrophobicities of the conjugates by attaching different alkyl groups with varying chain lengths. The synthesis was straightforward, with no practical surprises. The conjugates were obtained in moderate to good yields, and were easily purified using RP-HPLC. All the conjugates were characterized beyond doubt.

One of our major goal was to retain all the chelation properties of the original siderophore in the conjugates. In this study, we have shown that conjugation to imidazole did not alter either the iron binding stoichiometry or the binding equilibria of DFO. This invariably proved that imidazole part of the conjugate did not offer any extra binding site. In

1 the DPPH-assay, the conjugates were able to scavenge DPPH radical, proving their
2 antioxidant capabilities. The DPPH scavenging ability of DFO has been reported earlier.^{14,46}
3
4 The iron chelators, DFO and the conjugates **I-IV**, contain hydroxamate groups which can
5 donate a hydrogen atom to DPPH radical, resulting in the scavenging of DPPH radical
6 alongwith the formation of a stable nitroxide radical.⁴⁷ The scavenging abilities of the
7 conjugates, and thereby the antioxidant properties, were comparable with that of DFO.
8
9

10
11
12
13
14
15 Iron overload is a concern in a number of clinical conditions, as excess cellular iron
16 facilitates pro-oxidant reactions with oxygen or nitrogen substrates, giving rise to oxidative
17 stress.⁴⁸ Diseases such as hereditary hemochromatosis or thalassemia are characterized by
18 non-localized deposits of excess iron, however a number of conditions are known in which
19 iron overload is circumscribed to a specific tissue or organelle (neurodegeneration with brain
20 iron accumulation, hereditary X-linked sideroblastic anemia, anemia of chronic disease.⁴⁹
21 Patients of FA typically have a decreased expression of the peptide frataxin, which assists the
22 assembly of iron-sulfur clusters within the cell. Clinically relevant chelators must halt this
23 oxidation. For this, development of cell-permeable chelators is of urgent need. In our study,
24 we have demonstrated that increased hydrophobicity, synergised with a charged moiety, help
25 the chelator to penetrate cells.
26
27
28
29
30
31
32
33
34
35
36
37
38
39

40 A combination of electrostatic, dispersion interactions, hydrophobic effects, and
41 hydrogen bonds dynamics at the interface account for the overall mechanisms of interaction
42 of an imidazolium salt with biomenbranes.⁵⁰ The basic structures of all biomembranes are
43 formed by phospholipid bilayer, with hydrophilic negatively charged phosphate head and a
44 hydrophobic tail consisting of two fatty acid chains. The absence of an imidazolium cation in
45 conjugate **I** is responsible for its decreased cell permeability, mainly because the electrostatic
46 interaction of imidazolium cation with the negative charge groups in the lipid head is
47 diminished in conjugate **I** compared to that of conjugate **IV**, despite both having similar
48 hydrophobicities. Among the conjugates **II**, **III** and **IV**, the degree of cellular internalization
49
50
51
52
53
54
55
56
57
58
59
60

1 is dependent on the alkyl chain length as reported earlier.⁵¹ The hydrophobic alkyl chains
2 have been demonstrated to internalise *via* hydrophobic interactions through membrane
3 curvature. Recently, Durand et. al.⁵² have shown the effect of alkyl chain length in the
4 membrane interactions of phenolipids. According to their study, C8-alkyl chain substituted
5 molecules show the highest penetration depth. This corroborates with our finding that
6 molecule **IV** shows the highest penetration and chelation of LIP in cancer cells. In fact,
7 conjugate **IV** showed almost complete fluorescence recovery in our experiments, suggesting
8 a high degree of localisation of **IV** inside the cells.
9

10 Biologically, cellular uptake of various metabolites and substances is mediated
11 primarily through two receptor dependent endocytosis process.⁵³ These two processes is
12 regulated *via* clathrin and caveolae. Besides, cell also employs a non-specific and receptor
13 independent macropinocytosis process for internalizing various types of substances. In our
14 study, sucrose treatment, which inhibits clathrin-mediated endocytosis due to hypertonic
15 condition, partially reduced LIP chelation by compound **IV** in cells. Similarly, nystatin,
16 which inhibits lipid rafts caveolae mediated endocytosis, also partially reduced LIP chelation
17 by compound **IV** in cells. However, the extent of inhibitory effects of sucrose and nystatin
18 were weak, suggested an existence of alternate mode of cellular uptake for compound **IV**.
19 Apart from receptormediated endocytosis, a non-specific and receptor independent
20 macropinocytosis process is known to internalize various substances.^{41,53} Since
21 macropinocytosis process is dependent crucially on actin polymerization and membrane
22 ruffling, a microtubule and actin organization disrupting agent such as nocodazole has been
23 used for inhibition of macropinocytosis. Intriguingly, cells treated with nocodazole
24 significantly reduced LIP chelation by compound **IV**. Together, our results suggested that
25 cellular uptake compound **IV** is initially starts with ionic and C8-chain mediated chemical
26 interaction with membrane phospholipids and subsequently it may be internalized through
27 both receptor-dependent endocytosis and receptor-independent macropinocytosis process. At
28
29
30
31
32
33
34
35
36
37
38
39
40
41
42
43
44
45
46
47
48
49
50
51
52
53
54
55
56
57
58
59
60

1 present, it is unclear whether endocytosis and macropinocytosis processes for cellular uptake
2
3 of compound **IV** act cooperatively or not. It warrants further studies to unravel the molecular
4
5 mechanism of cellular internalization of compound **IV**.
6
7

8 Number of evidences has been reported till date⁵⁴⁻⁵⁷ to link iron overload to the
9
10 growth of cancer and related metastasis. Since neoplastic cells require more iron, cell-
11
12 permeable iron chelators have been projected as potential candidates for use in adjunctive
13
14 therapy in iron-overloaded cancers. Although DFO has been seen to disrupt intracellular iron
15
16 homeostasis, it acts only at a higher dose, and did not show any substantial effect at lower
17
18 doses. This is due to the high hydrophilicity of DFO, which inhibits it to chelate intracellular
19
20 iron, and therefore has not been much used as adjuvant in iron-overloaded cancers. In
21
22 contrast, compound **IV** has been shown to be cell-permeable and highly effective in chelating
23
24 LIP in the current study. Therefore, compound **IV**, as an adjuvant with chemo/radiation
25
26 therapy for iron overloaded cancer, may enhance the therapeutic outcomes.
27
28
29
30
31
32

33 **Conclusion**

34
35 In conclusion, we have demonstrated that the conjugates **I-IV** retained the iron chelation
36
37 abilities of DFO, but at the same time conjugate **IV** showed significant enhancement in its
38
39 cell penetration efficiency. Besides its use in iron overload diseases, this property of
40
41 imidazolium cations with desired hydrophobicity can be used in drug delivery, particularly as
42
43 small molecule based vector. The possibility of using compound **IV** as an adjuvant in cancer
44
45 therapy and other diseases will be explored in future.
46
47
48
49
50
51

52 **EXPERIMENTAL SECTION**

53 *General Chemistry*

54 All chemicals (AR grade) were purchased from Sigma-Aldrich, and were used without
55
56 further purification. All solvents (AR grade) used for synthesis were purchased from SRL,
57
58
59
60

1 India. Unless otherwise mentioned, HBS (NaCl 150 mM, HEPES 20 mM; pH 7.4; treated
2 with Chelex-100 purchased from Sigma, 1 g/100 mL) was used throughout the experiments.
3
4 Phosphate Buffer Saline (PBS) was prepared with 0.14 mol L⁻¹ NaCl; 2.6 mmol L⁻¹ NaH₂PO₄
5
6 H₂O and 7.4 mmol L⁻¹ Na₂HPO₄·7H₂O, pH 7.4. For characterization, the IR spectra (KBr)
7
8 were recorded with a BRUKER Tensor II spectrophotometer. The ¹H and ¹³C NMR spectra
9
10 were recorded with a Bruker AC-200 (200 MHz) or a Varian 500 MHz NMR spectrometer,
11
12 and the NMR spectra were processed using either MestReNova Lite-11.0.4, ACD/1D NMR
13
14 Processor or Bruker TOPSPIN software. The elemental analyses were carried with an
15
16 Elementar Vario micro cube. The logP_{OW} (octanol/water) of all the conjugates **I-IV** were
17
18 calculated using MarvinSketch 18.4.0 (ChemAxon Ltd.). UV-VIS electronic spectra were
19
20 recorded with commercial UV/VIS spectrophotometer (JASCO, V-550).
21
22
23
24
25

26 *Ethylimidazol-1-yl-acetate (2)*²²

27
28 K₂CO₃ (9.13 g, 66.09 mmol) and KOH (3.09 g, 55.09 mmol) were added
29
30 simultaneously to a solution of imidazole **1** (3.0 g, 44.07 mmol) in dry DCM (15 mL). The
31
32 suspension was stirred for 15 min. Thereafter, ethyl bromoacetate (6.09 mL, 55.09 mmol) and
33
34 a catalytic amount (10 mol %) of TBAI were added to it. The reaction was stirred at 25 °C for
35
36 8 h. On completion (*cf* TLC), the reaction mixture was filtered, residue washed with CHCl₃
37
38 and the filtrate was concentrated under vacuum. Purification by column chromatography
39
40 using 0-5% MeOH/CHCl₃ yielded **2** (2.65 g, 39%). Yellow oil; ¹H NMR (500 MHz, CDCl₃):
41
42 δ 1.27 (t, *J* = 7.0 Hz, 3H), 4.22 (q, *J* = 7.0 Hz, 2H), 4.68 (s, 2H), 6.94 (s, 1H), 7.07 (s, 1H),
43
44 7.49 (s, 1H). ¹³C NMR (125 MHz, CDCl₃): δ 14.0, 47.9, 61.9, 120.0, 129.4, 137.9, 167.5.
45
46
47
48
49

50 *5.3. 1H-Imidazol-1-yl-acetic acid hydrochloride (3)*²³

51
52 A solution of **2** (0.79 g, 5.12 mmol) in 40% aqueous HCl (10 mL) was refluxed for 4
53
54 h. After completion of reaction (*cf* TLC), water was removed under vacuum, and column
55
56 chromatography of the residue using 0-50% MeOH/CHCl₃ yielded pure **3** (0.80 g, 96%).
57
58 White solid; m.p. 202-206 °C (decom.) [Lit²³ m.p. 206.6-207.6 °C]; ¹H NMR (500 MHz, D₂O):
59
60

1 δ 5.18 (s, 2H), 7.52 (s, 1H), 7.54 (s, 1H), 8.82 (s, 1H); ^{13}C NMR (125 MHz, D_2O): δ 49.7,
2
3
4 119.6, 123.1, 135.9, 170.0.

5
6 *1H-Imidazole-1-acetic acid-DFO conjugate (I)*

7
8 A suspension of **3** (0.05 g, 0.31 mmol), DFO-Mes (0.20 gm, 0.31 mmol), DIC (0.06
9 mL, 0.39 mmol) and HOBt (0.05 g, 0.39 mmol) in 10 ml DMF was heated under N_2
10 atmosphere at 45°C for 1 h. After 1 h, the reaction mixture was cooled to room temperature,
11 and DIPEA (0.15 mL, 0.88 mmol) was added to it. The reaction mixture was stirred for 8 h.
12 Solvent removal under vacuum yielded a solid residue, which was washed with EtOAc (3 x
13 10 mL) and was dissolved in water. The water extract was concentrated under vacuum. ^1H
14 NMR of the crude solid confirmed the presence of the conjugate **I**. Purification of the crude
15 residue by semi-preparative RP-HPLC yielded pure **I** (yield 0.148 g, 72%) light yellow solid.
16
17 ^1H NMR (500 MHz, DMSO-d_6): δ 1.17-1.28 (m, 6H), 1.31-1.41 (m, 6H), 1.42-1.51 (m, 6H),
18 1.97 (s, 3H), 2.27-2.35 (m, 4H), 2.58-2.67 (m, 4H), 2.89-3.09 (m, 6H), 3.42-3.48 (m, 6H),
19 4.61 (s, 2H), 6.86 (s, 1H), 7.03 (s, 1H), 7.58 (s, 1H), 7.69 (broad s, 3H), 8.01-8.09 (m, 3H).
20
21 Anal. Calcd for $\text{C}_{30}\text{H}_{52}\text{N}_8\text{O}_9$: C, 53.88; H, 7.84; N, 16.75. Found: C, 53.64; H, 7.68; N, 16.98.

22
23
24
25
26
27
28
29
30
31
32
33
34
35
36 *N-butyl imidazole (5)*

37
38 K_2CO_3 (15.23 g, 110.17 mmol) and KOH (4.95 g, 88.14 mmol) were added to a
39 solution of imidazole **1** (5.0 g, 73.45 mmol) in dry DCM (25 mL) and stirred for 15 minutes.
40 To this suspension, 1-bromo butane (11.89 ml, 110.17 mmol) and a catalytic amount (10 mol
41 %) of TBAI was added. The reaction was stirred for 6 h. On completion (*cf* TLC), the
42 reaction mixture was filtered, residue washed with CHCl_3 and the filtrate was concentrated
43 under vacuum. Purification by column chromatography using 0-5% MeOH/ CHCl_3 yielded **5**
44 (6.5 g, 71%). Yellow oil; ^1H NMR (500 MHz, DMSO-d_6): δ 0.86 (t, $J = 7.5$ Hz, 3H), 1.16-
45 1.24 (m, 2H), 1.62-1.68 (m, 2H), 3.93 ((t, $J = 7.5$ Hz, 2H), 6.86 (s, 1H), 7.13 (s, 1H), 7.59 (s,
46 1H); ^{13}C NMR (125 MHz, DMSO-d_6): δ 13.8, 19.6, 33.1, 46.1, 119.6, 128.7, 137.6. Anal.
47
48 Calcd for $\text{C}_7\text{H}_{12}\text{N}_2$: C, 67.70; H, 9.74; N, 22.56. Found: C, 67.77; H, 9.87; N, 22.87.

N-octyl imidazole (**6**)

As described previously, K₂CO₃ (15.23 g, 110.17 mmol) and KOH (4.95 g, 88.14 mmol) were added to a solution of imidazole **1** (5.0 g, 73.45 mmol) in dry DCM (25 mL) and stirred for 15 minutes. To this suspension, 1-bromo octane (19.03 mL, 110.17 mmol) and a catalytic amount (10 mol%) of TBAI was added. The reaction was stirred overnight. On completion (*cf* TLC), the reaction mixture was filtered, residue washed with CHCl₃ and the filtrate was concentrated under vacuum. Purification by column chromatography using 0-5% MeOH/CHCl₃ yielded **6** (9.9 g, 75%). Yellow oil; ¹H NMR (500 MHz, CDCl₃): δ 0.87 (t, *J* = 7.0 Hz, 3H), 1.24-1.28 (m, 10H), 1.74-1.77 (m, 2H), 3.91 (t, *J* = 7.0 Hz, 2H), 6.89 (s, 1H), 7.04 (s, 1H), 7.45 (s, 1H). ¹³C NMR (125 MHz, CDCl₃): δ 14.0, 22.5, 26.5, 28.9, 29.0, 31.0, 31.6, 46.9, 118.7, 129.2, 137.0. Anal. Calcd for C₁₁H₂₀N₂: C, 73.28; H, 11.18; N, 15.54. Found: C, 73.09; H, 11.32; N, 15.36.

1-methyl-3-(2-ethoxy-2-oxoethyl)-imidazolium bromide (**7**)

Ethyl bromoacetate (5.5 mL, 50.06 mmol) was added dropwise to a pre-cooled (-10 °C) solution of **4** (4.11 g, 50.06 mmol) in dry THF (25 ml). The reaction was gradually brought to room temperature and was stirred overnight. Solvent evaporation followed by washing of the residue with Et₂O (3 x 10 mL) and drying under vacuum yielded pure **7** (8.50 g, 68%). Yellow viscous oil; ¹H NMR (200 MHz, CDCl₃): δ 1.14 (t, *J* = 7.0 Hz, 3H), 3.95 (s, 3H), 4.10 (q, *J* = 7.2 Hz, 2H), 5.34 (s, 2H), 7.58 (d, *J* = 1.6 Hz, 1H), 7.67 (d, *J* = 1.8 Hz, 1H), 9.79 (t, *J* = 1.8 Hz, 1H); ¹³C NMR (50 MHz, CDCl₃): δ 14.0, 36.9, 50.2, 62.8, 123.2, 123.9, 137.9, 166.2.

5.8. 1-butyl-3-(2-ethoxy-2-oxoethyl)-imidazolium bromide (**8**)

Ethyl bromoacetate (5.5 mL, 49.93 mmol) was added dropwise to a pre-cooled (-10 °C) solution of **5** (6.2 g, 49.93 mmol) in dry THF (25 ml). The reaction was gradually brought to room temperature and was stirred overnight. Solvent evaporation followed by washing of the residue with Et₂O (3 x 10 mL) and drying under vacuum yielded pure **8** (9.48 g, 65%).

1 Yellow viscous oil; ^1H NMR (500 MHz, CDCl_3): δ 0.88 (t, $J = 7.5$ Hz, 3H), 1.22 (t, $J = 7.0$
2 Hz, 3H), 1.28-1.33 (m, 2H), 1.81-1.87 (m, 2H), 4.17 (q, $J = 7.0$ Hz, 2H), 4.26 (t, $J = 7.5$ Hz,
3 4 Hz, 2H), 5.43 (s, 2H), 7.52 (s, 1H), 7.72 (s, 1H), 10.12 (s, 1H); ^{13}C NMR (125 MHz, CDCl_3): δ
5 6 7 13.4, 14.0, 19.3, 31.9, 50.0, 50.2, 62.8, 121.7, 124.0, 137.6, 166.1.

5.9. *1-octyl-3-(2-ethoxy-2-oxoethyl)-imidazolium bromide (9)*

12 Ethyl bromoacetate (1.3 mL, 11.48 mmol) was added dropwise to a pre-cooled (-10
13 $^{\circ}\text{C}$) solution of **6** (2.07 g, 11.48 mmol) in dry THF (15 ml). The reaction was gradually
14 brought to room temperature and was stirred overnight. Solvent evaporation followed by
15 washing of the residue with Et_2O (3 x 10 mL) and drying under vacuum yielded pure **9** (2.19
16 g, 55%). Yellow viscous oil; ^1H NMR (500 MHz, CDCl_3): δ 0.83 (t, $J = 7.0$ Hz, 3H), 1.18-
17 1.30 (m, 13H), 1.85-1.91 (m, 2H), 4.20-4.29 (m, 4H), 5.47 (s, 2H), 7.43 (s, 1H), 7.68 (s, 1H),
18 10.13 (s, 1H); ^{13}C NMR (125 MHz, CDCl_3): δ 13.9, 22.4, 26.0, 28.7, 28.8, 30.0, 31.5, 50.2,
19 62.7, 121.4, 123.9, 137.7, 166.0.

1-methyl-3-(carboxymethyl)-imidazolium bromide (10)

20 A solution of **7** (8.0 g, 32.11 mmol) in 40% aqueous HCl was refluxed for 4 h. After
21 the reaction was complete (*cf* TLC), water was removed under vacuum to yield pure **10** (5.76
22 g, 81%). Yellow viscous oil; ^1H NMR (500 MHz, D_2O): δ 3.88 (s, 3H), 5.06-5.13 (m, 2H),
23 7.44-7.46 (m, 2H), 8.76 (s, 1H); ^{13}C NMR (125 MHz, DMSO-d_6): δ 36.1, 50.0, 123.5, 137.3,
24 170.0. Anal. Calcd for $\text{C}_6\text{H}_9\text{BrN}_2\text{O}_2$: C, 32.60; H, 4.10; N, 12.67. Found: C, 32.54; H, 4.36;
25 26 27 28 29 N, 12.68.

1-butyl-3-(carboxymethyl)-imidazolium bromide (11)

30 A solution of **8** (9.18 g, 31.53 mmol) in 40% aqueous HCl (30 mL) was refluxed for 4
31 h. After the reaction was complete (*cf* TLC), water was removed under vacuum to yield pure
32 **11** (7.17g, 86%). Yellow viscous oil; ^1H NMR (500 MHz, DMSO-d_6): δ 0.87 (t, $J = 7.5$ Hz,
33 3H), 1.20-1.25 (m, 2H), 1.73-1.78 (m, 2H), 4.26 (t, $J = 7.0$ Hz, 2H), 5.21 and 5.34 (two s,
34 35 36 37 38 39 40 41 42 43 44 45 46 47 48 49 50 51 52 53 54 55 56 57 58 59 60 2H), 7.82 (s, 1H), 7.90 (s, 1H), 9.37 (s, 1H); ^{13}C NMR (125 MHz, DMSO-d_6): δ 13.7, 19.1,

1 31.8, 49.2, 53.3, 122.6, 124.3, 137.6, 167.8. Anal. Calcd for C₉H₁₅BrN₂O₂: C, 41.08; H, 5.75;
2
3
4 N, 10.65. Found: C, 40.90; H, 6.32; N, 10.28.

5
6 *1-octyl-3-(carboxymethyl)-imidazolium bromide (12)*
7

8 A solution of **9** (2.0 g, 5.76 mmol) in 40% aqueous HCl was refluxed for 4 h. After
9
10 the reaction was complete (*cf* TLC), water was removed under vacuum to yield pure **12** (1.51
11
12 g, 82%). Light brown solid; ¹H NMR (500 MHz, D₂O): δ 0.74 (t, *J* = 6.5 Hz, 3H), 1.14-1.19
13
14 (m, 10H), 1.76-1.79 (m, 2H), 4.13 (t, *J* = 7.0 Hz, 2H), 4.99 (s, 2H), 7.41 (s, 1H), 7.44 (s, 1H),
15
16 8.75 (s, 1H); ¹³C NMR (125 MHz, D₂O): δ 13.4, 22.0, 25.2, 27.9, 28.1, 29.0, 30.9, 49.9, 50.1,
17
18 122.3, 123.6, 136.6, 170.1. Anal. Calcd for C₁₃H₂₃BrN₂O₂: C, 48.91; H, 7.26; N, 8.78. Found:
19
20 C, 48.44; H, 7.52; N, 8.54.
21
22

23
24 *1-methyl-3-(carboxymethyl)-imidazolium-DFO conjugate (II)*
25

26 A suspension of **10** (0.155 g, 0.70 mmol), DFO-Mes (0.46 gm, 0.70 mmol), DIC (0.14
27
28 mL, 0.90 mmol) and HOBt (0.12 g, 0.90 mmol) in 10 ml DMF was heated under N₂
29
30 atmosphere at 50 °C for 1 h. After 1 h, the reaction mixture was cooled to room temperature,
31
32 and DIPEA (0.37 mL, 2.1 mmol) was added to it. The reaction mixture was stirred overnight.
33
34 Solvent removal under vacuum yielded a solid residue, which was washed with EtOAc (3 x
35
36 10 mL) and was dissolved in water. The water extract was concentrated under vacuum. ¹H
37
38 NMR of the crude solid confirmed the presence of the conjugate **II**. ¹H NMR of the crude
39
40 solid confirmed the presence of the conjugate **II**. Purification of the crude residue by semi-
41
42 preparative RP-HPLC yielded pure **II** (yield 0.371 g, 68%) light yellow solid. ¹H NMR (200
43
44 MHz, D₂O): 1.20-1.41 (m, 6H), 1.53-1.57 (m, 6H), 1.64-1.68 (m, 6H), 2.12 (s, 3H), 2.47-2.50
45
46 (m, 4H), 2.72 (s, 3H), 2.77-2.81 (m, 4H), 3.16-3.18 (m, 4H), 3.19-3.20 (m, 1H), 3.33-3.34
47
48 (m, 1H), 3.60-3.64 (m, 6H), 3.99 (two s merged together, 3H), 5.03 (s, 2H), 7.54-7.57 (m,
49
50 1H), 7.62 (s, 1H), 8.98 (s, 1H). Anal. Calcd for C₃₂H₅₈N₈O₁₂S: C, 49.34; H, 7.51; N, 14.39; S,
51
52 4.12. Found: C, 49.06; H, 7.48; N, 14.75; S, 3.74.
53
54
55
56
57

58
59 *1-butyl-3-(carboxymethyl)-imidazolium-DFO conjugate (III)*
60

1 A suspension of **11** (0.185 g, 0.70 mmol), DFO-Mes (0.46 gm, 0.70 mmol), DIC (0.14
2 mL, 0.90 mmol) and HOBt (0.12 g, 0.90 mmol) in 10 ml DMF was heated under N₂
3 atmosphere at 50 °C for 1 h. After 1 h, the reaction mixture was cooled to room temperature,
4 and DIPEA (0.37 mL, 2.10 mmol) was added to it. The reaction mixture was stirred
5 overnight. Solvent removal under vacuum yielded a solid residue, which was washed with
6 EtOAc (3 x 10 mL) and was dissolved in water. The water extract was concentrated under
7 vacuum. ¹H NMR of the crude solid confirmed the presence of the conjugate **III**. Purification
8 of the crude residue by semi-preparative RP-HPLC yielded pure **III** (yield 0.380 g,
9 66%).yellow solid. ¹H NMR (500 MHz, DMSO-d₆): δ 0.89 (t, *J* = 7.5 Hz, 3H), 1.20-1.26 (m,
10 8H), 1.35-1.38 (m, 6H), 1.48-1.50 (m, 6H), 1.75-1.78 (m, 2H), 1.95 (s, 3H), 2.25-2.30 (m,
11 4H), 2.55-2.59 (m, 4H), 2.72-2.76 (m, 1H), 2.96-3.00 (m, 6H), 3.42-3.47 (m, 8H), 4.19-4.20
12 (m, 2H), 4.84 (s, 1H), 4.95 (s, 1H), 7.67-7.76 (m, 5H), 9.11-9.15 (m, 1H), 9.62-9.67 (m, 3H).
13 Anal. Calcd for C₃₅H₆₄N₈O₁₂S: C, 51.20; H, 7.86; N, 13.65; S, 3.91. Found: C, 50.81; H,
14 7.74; N, 13.96; S, 4.17.

15
16
17
18
19
20
21
22
23
24
25
26
27
28
29
30
31
32
33
34 *1-Octyl-3-(carboxymethyl)-imidazolium-DFO conjugate (IV)*

35 A suspension of **12** (0.115g, 0.36mmol), DFO-Mes (0.24g, 0.36 mmol), DIC (0.07ml,
36 0.45mmol) and HOBt (0.06g, 0.45mmol) in 10 ml DMF was heated under N₂ atmosphere at
37 50 °C for 1 h. After 1 h, the reaction mixture was cooled to room temperature, and DIPEA
38 (0.19 ml, 1.08 mmol) was added to it. The reaction mixture was stirred overnight. Solvent
39 removal under vacuum yielded a solid residue, which was washed with EtOAc (3 x 10 mL),
40 water (3 x 10 mL) and MeOH (3 x 10 mL). The methanol extract was concentrated under
41 vacuum. ¹H NMR of the crude solid confirmed the presence of the conjugate **IV**. Purification
42 of the crude residue by semi-preparative RP-HPLC yielded pure **IV** (yield 0.224 g, 71%).
43 yellow solid. ¹H NMR (500 MHz, DMSO-d₆): δ 0.84 (t, *J* = 7.0 Hz, 3H), 1.15-1.26 (m, 16H),
44 1.35-1.39 (m, 6H), 1.42-1.49 (m, 6H), 1.75-1.79 (m, 2H), 1.95 (s, 3H), 2.25-2.29 (m, 4H),
45 2.30-2.32 (m, 2H), 2.57-2.60 (m, 4H), 2.73-2.76 (m, 1H), 3.00-3.12 (m, 6H), 3.42-3.47 (m,
46
47
48
49
50
51
52
53
54
55
56
57
58
59
60

1 6H), 4.18 (t, $J = 7.0$ Hz, 2H), 4.94 (s, 2H), 7.66-7.76 (m, 4H), 8.38 (s, 1H), 9.11 (s, 1H), 9.58-
2
3 9.65 (m, 3H). Anal. Calcd for $C_{39}H_{72}N_8O_{12}S$: C, 53.41; H, 8.27; N, 12.78; S, 3.66. Found: C,
4 53.12; H, 8.62; N, 12.95; S, 3.64.
5
6

7 *Binding stoichiometry*

8
9

10 The solutions of FAS, DFO and conjugates **I-IV** (100 μ M each in 10% DMSO) were
11 freshly prepared. FAS solution was mixed with the solutions of the conjugates **I-IV** (or DFO)
12 and were allowed to equilibrate for 30 min. The electronic spectra were recorded at 30 $^{\circ}$ C. For
13 Job's plot, the electronic spectra of Fe-chelator (DFO or conjugates **I-IV**) solutions with
14 varying mole fractions (iron mole fractions ranging from 0-0.8) were recorded at 30 $^{\circ}$ C.
15
16
17
18
19
20
21

22 *Competition studies with calcein*

23

24 190 μ L of 2 μ M calcein (in HBS, pH 7.4) were placed in each well of a flat, transparent 96-
25 well microplate. Fluorescence was recorded at 37 $^{\circ}$ C on a mutliwell fluorescence plate reader
26 (Tecan Infinite M200, Switzerland, $\lambda_{exc}/\lambda_{em} = 485/520$ nm) for 10 min (till stabilization of
27 fluorescence). After that, 10 μ L of 40 μ M FAS (instantly prepared in water, final concentration
28 2 μ M) was added in each well, and was allowed to react at 37 $^{\circ}$ C for 10 min. Thereafter,
29 fluorescence was recorded until stabilization (~ 10 min). The calcein-Fe (CAFe) solutions
30 formed in the wells were treated with increasing concentrations (0-24 μ M of the compounds
31 **I-IV** (10 μ L aliquots), and fluorescence was further recorded (~ 60 min).
32
33
34
35
36
37
38
39
40
41
42

43 *Competition studies with fluorescein-apotransferrin*

44

45 180 μ L of 2 μ M FITf solution (in HBS, pH 7.4) was placed in each well of a flat,
46 transparent 96-well microplate, and the fluorescence was recorded at 37 $^{\circ}$ C on a mutliwell
47 fluorescence plate reader (Tecan Infinite M200, Switzerland) for 10 min (till stabilization).
48 After that, 10 μ L of 4 μ M FAS (instantly prepared in water, final concentration) was added to
49 each well, and fluorescence was recorded till stabilization of fluorescence quenching (~ 10
50 min). Next, the solutions were treated with increasing concentrations (0-20 μ M) of chelators
51
52
53
54
55
56
57
58
59
60

1 (I-IV) (10 μ L aliquots), and the fluorescence was further recorded until stabilization (~60
2
3
4 min).

5 6 *DPPH assay*

7
8 Aliquots of 120 μ L of 0.1 mM DPPH (in methanol) was placed in flat, transparent 96-
9
10 well microplates. To that, 60 μ L of HBS/Chelex buffer was added. Next, the solutions were
11
12 treated with increasing concentrations (0–100 μ M) of conjugates I-IV (10 μ L aliquots,
13
14 solutions prepared in H₂O/DMSO). The mixtures were incubated for 30 min at 37 °C in the
15
16 dark. Absorbance at 520 nm was then recorded.
17
18

19 20 *Cell permeation and intracellular iron chelation assay*

21
22 In order to study cell permeation and intracellular iron chelation potential of DFO or
23
24 conjugates I-IV, a flow cytometry based assay in U2-OS (Osteosarcoma) cells was used. U2-
25
26 OScells (0.1 \times 10⁶ cells/well, 6 well plate) were grown in DMEM medium supplemented
27
28 with 10% heat-inactivated FBS, glutamine (2 mM), penicillin 100 U/ml, and streptomycin
29
30 (100 μ g/ml) in a humidified 5% CO₂ atmosphere at 37 °C for 24 h. Cells were washed with
31
32 PBS and supplemented with DMEM medium containing calcein-AM (200 nM, Sigma, St.
33
34 Louis, MO) for 30 min. Further, cell was washed with PBS, to remove extra-cellular calcein-
35
36 AM, and treated with DMEM medium containing FAS (50 μ M) and ascorbic acid (200 μ M)
37
38 for 30 min. Subsequently, cells were washed to remove extra-cellular iron, and treated with
39
40 DMEM medium containing DFO (100 μ M) or conjugates I-IV (10-100 μ M) for 60 min.
41
42 Cells were collected by trypsinization, washed two times with cold PBS and analyzed by
43
44 flow cytometry. Cellular debris was excluded from the analyses by raising the forward scatter
45
46 threshold. At least 2 \times 10⁴ cells of each sample were analyzed, and the data were registered
47
48 on a logarithmic scale. The calcein fluorescence in cells, expressed in arbitrary MFI units,
49
50 were analyzed by acquiring fluorescence (excitation at 480 nm and emission at 530 nm) in
51
52 FL1 channel in flow cytometer.³⁹ The difference in the MFI in absence and presence of
53
54 chelator represents ΔF , which was used as a measure of LIP. In some experiments, ΔF was
55
56
57
58
59
60

1 measured in the absence and presence of inhibitors (sucrose, nystatin and nocodazole). All
2
3 the flow cytometry analyses were carried out with a Pertec CyFlow® Space flow cytometer
4
5 using the FlowJo software. U2-OS cells were obtained from American Type Culture
6
7 Collection, VA USA.
8
9

10 *Cytotoxicity assay:*

11
12 The cytotoxic properties of compound **I-IV** and DFO was assessed by as per reported
13
14 MTT assay.⁵⁸
15
16

17 **Associated content**

18
19
20 **Supporting Information.** NMR spectra of all the compounds related to this article. This
21
22 material is available free of charge via the Internet at <http://pubs.acs.org>.
23
24

25 **Author information**

26
27
28 Corresponding Author*

29
30
31 E-mail: dibakarg@barc.gov.in; Phone: + 91 2559 2408; fax: +91 2550 5151.
32
33

34 **Notes**

35
36
37 The authors declare no competing financial interest.
38
39

40 **Acknowledgments**

41
42
43 We thank Dr. Manoj Kumbhakar, RPCD, BARC for his help and guidance during the UV
44
45 experiments and during the preparation of the manuscript.
46
47

48 **Abbreviations**

49
50
51 DIC, N,N'-diisopropylcarbodiimide; HOBt, N-hydroxybenzotriazole; DIPEA,
52
53 diisopropylamine; DCM, dichloromethane; MeOH, methanol; DMSO, dimethyl sulfoxide;
54
55 DMF, N,N'-dimethylformamide; ACN, acetonitrile; FAS, ferrous ammonium sulfate; HBS,
56
57 HEPES buffered saline; PBS, Phosphate buffer saline; 5-DTAF, 5-(4,6-dichlorotriazinyl)
58
59 aminofluorescein; DPPH, 2,2-diphenyl-1-picrylhydrazyl.
60

References

1. Abbaspour, N., Hurrell, R., Kelishadi, R. (2014) Review on iron and its importance for human health. *J. Res. Med. Sci.* 19, 164-174.
2. Waldvogel-Abramowski, S., Waeber, G., Gassner, C., Buser, A., Frey, B. M., Favrat, B., Tissot, J. D. (2014) Physiology of iron metabolism. *Transfus. Med. Hemother.* 41, 213-221.
3. Andrews, N. C., Schmidt, P. J. Iron homeostasis. *Annu. Rev. Physiol.* 69, 69-85.
4. Goswami, D., Machini, M. T., Silvestre, D. M., Nomura, C. S., Esposito, B. P. (2014) Cell penetrating peptide (CPP)-conjugated desferrioxamine for enhanced neuroprotection: synthesis and in vitro evaluation. *Bioconjugate Chem.* 25, 2067-2080, and references cited therein.
5. Guidelines for the clinical management of thalassaemia [Internet] (2008) (Cappellini, M. D., Cohen, A., Eleftheriou, A., Piga, A., Porter, J., and Taher, A. Eds.) 2nd Revised edition. Nicosia (CY): Thalassaemia International Federation;
6. Sheth, S. Iron chelation: an update. (2014) *Curr. Opin. Hematol.* 21, 179-185.
7. Borgna-Pignatti, C., Rugolotto, S., De Stefano, P.; Zhao, H., Cappellini, M. D., Del Vecchio, G. C., Romeo, M. A., Forni, G. L., Gamberini, M. R., Ghilardi, R., Piga, A., Cnaan, A. (2004) Survival and complications in patients with thalassemia major treated with transfusion and deferoxamine. *Haematologica* 89,1187-1193.
8. Gumienna-Kontecka, E., Nurchi, V. M., Szebesczyk, A., Bilaska, P., Krzywoszynska, K., Kozlowski, H. (2013) Chelating agents as tools for the treatment of metal overload. *Z. Anorg. Allg. Chem.* 639,1321-1331.
9. Thuret, I. (2013) Post-transfusional iron overload in the haemoglobinopathies. *Comptes Rendus Biologies* 336, 164-172.

- 1
2
3
4
5
6
7
8
9
10
11
12
13
14
15
16
17
18
19
20
21
22
23
24
25
26
27
28
29
30
31
32
33
34
35
36
37
38
39
40
41
42
43
44
45
46
47
48
49
50
51
52
53
54
55
56
57
58
59
60
10. Poggiali, E., Cassinerio, E., Zanaboni, L., Cappellini, M. D. (2012) An update on iron chelation therapy. *Blood Transfus.* 10, 411-422.
11. Hider, R. C., Zhou, T. (2005) The design of orally active iron chelators, *Ann. N. Y. Acad. Sci.* 1054, 141-154.
12. Chaston, T. B., Richardson, D. R. (2003) Iron chelators for the treatment of iron overload disease: relationship between structure, redox activity, and toxicity. *Am. J. Hematol.* 73, 200-210.
13. Liu, J., Obando, D., Schipanski, L.G., Groebler, L. K., Witting, P. K., Kalinowski, D. S., Richardson, D. R., Codd, R. (2010) Conjugates of desferrioxamine B (DFOB) with derivatives of adamantane or with orally available chelators as potential agents for treating iron overload. *J. Med. Chem.* 53, 1370-1382.
14. Alta, E. C. P., Goswami, D., Machini, M. T., Silvestre, D. M., Nomura, C. S., Espósito, B. P. (2014) Desferrioxamine-caffeine (DFCAF) as a cell permeant moderator of the oxidative stress caused by iron overload. *BioMetals* 27, 1351-1360.
15. Liu, X. S., Patterson, L. D., Miller, M. J., Theil, E. C. (2007) Peptides selected for the protein nanocage pores change the rate of iron recovery from the ferritin mineral. *J. Biol. Chem.* 282,31821-31825.
16. Alta, R. Y., Vitorino, H. A., Goswami, D., Liria, C. W., Wisnovsky, S. P., Kelley, S. O., Machini, M. T., Espósito, B. P. (2017) Mitochondria-penetrating peptides conjugated to desferrioxamine as chelators for mitochondrial labile iron. *PLoS One* 12, e0171729.
17. Alta, R. Y. P., Vitorino, H. A., Goswami, D., Machini, M. T., Espósito, B. P. (2017) Triphenylphosphonium-desferrioxamine as a candidate mitochondrial iron chelator. *Biometals* 30, 709-718.
18. Gotsbacher, M. P., Telfer, T. J., Witting, P. K., Double, K. L., Finkelstein, D. I., Codd, R. (2017) Analogues of desferrioxamine B designed to attenuate iron-mediated

- 1 neurodegeneration: synthesis, characterisation and activity in the MPTP-mouse model
2
3 of Parkinson's disease. *Metallomics* 9, 852-864.
4
5
- 6 19. Reinhardt, A., Horn, M., Pieper gen. Schmauck, J., Bröhl, A., Giernoth, R., Oelkrug,
7
8 C., Schubert, A., Neundorf, I. (2014) Novel imidazolium salt-peptide conjugates and
9
10 their antimicrobial activity. *Bioconjugate Chem.* 25, 2166-2174.
11
12
- 13 20. Egorova, K.S., Seitkalieva, M. M., Posvyatenko, A. V., Khrustalev, V. N., Ananikov,
14
15 V. P. (2015) Cytotoxic activity of salicylic acid-containing drug models with ionic
16
17 and covalent binding. *ACS Med. Chem. Lett.* 6, 1099-1104.
18
19
- 20 21. Cole, M. R., Li, M., El-Zahab, B., Janes, M. E., Hayes, D., Warner, I. M. (2011)
21
22 Design, synthesis, and biological evaluation of β -lactam antibiotic-based
23
24 imidazolium- and pyridinium-type ionic liquids. *Chem. Biol. Drug Des.* 78, 33-41.
25
26
- 27 22. Ratel, M., Provencher-Girard, A., Zhao, S. S., Breault-Turcot, J., Labrecque-
28
29 Carbonneau, J., Branca, M., Pelletier, J. N., Schmitzer, A. R., Masson, J. -F. (2013)
30
31 Imidazolium-based ionic liquid surfaces for biosensing. *Anal. Chem.* 85, 5770-5777.
32
33
- 34 23. Yang, G., Hu, X., Wu, Y., Liu, C., Zhang, Z. (2012) Phenol oxidation catalyzed by a
35
36 simple water-soluble copper catalyst with an imidazole salt tag. *Catal. Commun.* 26,
37
38 132-135.
39
- 40 24. Siebner-Freibach, H., Yariv, S., Lapidés, Y., Hadar, Y., Chen, Y. (2005) Thermo-
41
42 FTIR spectroscopic study of the siderophore ferrioxamine B: spectral analysis and
43
44 stereochemical implications of iron chelation, pH, and temperature. *J. Agric. Food*
45
46 *Chem.* 53, 3434-3443.
47
48
- 49 25. Yang, G., Chanthad, C., Oh, H., Ayhan, I. A., Wang, Q. (2017) Organic-inorganic
50
51 hybrid electrolytes from ionic liquid-functionalized octasilsesquioxane for lithium
52
53 metal batteries. *J. Mater. Chem. A* 5, 18012-18019.
54
55
56
57
58
59
60

- 1
2
3
4
5
6
7
8
9
10
11
12
13
14
15
16
17
18
19
20
21
22
23
24
25
26
27
28
29
30
31
32
33
34
35
36
37
38
39
40
41
42
43
44
45
46
47
48
49
50
51
52
53
54
55
56
57
58
59
60
26. Rahman, Md. T., Barikbin, Z., Badruddoza, A. Z. M., Doyle, P. S., Khan, S. A. (2013) Monodisperse polymeric ionic liquid microgel beads with multiple chemically switchable functionalities. *Langmuir* 29, 9535-9543.
27. Malek, K., Puc, A., Schroeder, G., Rybachenko, V. I., Proniewicz, L. M. (2006) FT-IR and FT-Raman spectroscopies and DFT modelling of benzimidazolium salts. *Chem. Phys.* 327, 439-451.
28. Vignessa, S., Sivashanmugama, A., Mohandasa, A., Janarthanan, R., Iyer, S., Nair, S. V., Jayakumar, R. (2018) Injectable deferoxamine nanoparticles loaded chitosan-hyaluronic acid coacervate hydrogel for therapeutic angiogenesis. *Colloids Surf. B Biointerfaces* 161,129-138.
29. Galla, F., Bourgeois, C., Lehmkuhl, K., Schepmann, D., Soeberdt, M., Lotts, T., Abels, C., Ständer, S., Wünsch, B. (2016) Effects of polar κ receptor agonists designed for the periphery on ATP-induced Ca^{2+} release from keratinocytes. *Med. Chem. Commun.* 7, 317-326.
30. Goodwin, J. F., Whitten, C. F. (1965) Chelation of ferrous sulphate solutions by desferrioxamine B. *Nature* 205, 281-283.
31. Ma, Y., Abbate, V., Hider, R. C. (2015) Iron-sensitive fluorescent probes: monitoring intracellular iron pools. *Metallomics* 7, 212-222.
32. Job, P. (1928) Formation and stability of inorganic complexes in solution. *Ann Chim France* 9,113–203.
33. Renny, J. S., Tomasevich, L. L., Tallmadge, E. H., Collum, D. B. (2013) Method of continuous variations: applications of Job plots to the study of molecular associations in organometallic chemistry. *Angew. Chem. Int. Ed.* 52, 11998-12013.
34. Ali, A., Zhang, Q., Dai, J., Huang, X. (2003) Calcein as a fluorescent iron chemosensor for the determination of low molecular weight iron in biological fluids. *Biometals* 16,285-293.

- 1
2
3
4
5
6
7
8
9
10
11
12
13
14
15
16
17
18
19
20
21
22
23
24
25
26
27
28
29
30
31
32
33
34
35
36
37
38
39
40
41
42
43
44
45
46
47
48
49
50
51
52
53
54
55
56
57
58
59
60
35. Espósito, B. P., Epsztejn, S., Breuer, W., Cabantchik, Z. I. (2002) A review of fluorescence methods for assessing labile iron in cells and biological fluids. *Anal. Biochem.* 304, 1-18.
 36. Cabantchik, Z. I., Glickstein, H., Milgram, P., Breuer, W. (1996) A fluorescence assay for assessing chelation of intracellular iron in a membrane model system and in mammalian cells. *Anal. Biochem.* 233, 221–227.
 37. Breuer, W., Cabantchik, Z. I. (2001) A fluorescence-based one-step assay for serum non-transferrin-bound iron. *Anal. Biochem.* 299,194-202.
 38. Kedare, S. B., Singh, R. P. (2011) Genesis and development of DPPH method of antioxidant assay. *J. Food Sci. Technol.* 48, 412-422.
 39. Prus, E., Fibach, E. (2008) Flow cytometry measurement of the labile iron pool in human hematopoietic cells. *Cytometry A.* 73,22-27.
 40. Epsztejn, S., Kakhlon, O., Glickstein, H., Breuer, W., Cabantchik, Z. I. (1997) Fluorescence analysis of the labile iron pool of mammalian cells. *Anal Biochem* 248, 31-40.
 41. Kee, S. H., Cho, E. J., Song, J. W., Park, K. S., Baek, L. J., Song, K. J. (2004) Effects of endocytosis inhibitory drugs on rubella virus entry into VeroE6 cells. *Microbiol Immunol.* 48, 823-829.
 42. Chutvanichkul, B., Vattanaviboon, P., Mas-oodi, S., U-pratya, Y., Wanachiwanawin, W. (2018) Labile iron pool as a parameter to monitor iron overload and oxidative stress status in b-thalassemic erythrocytes. *Cytometry, Part B* 94, 631–636.
 43. Izmaylov, B., Gioia, D. D., Markova, G., Aloisio, I., Colonna, M., Vasnev, V. (2015) Imidazolium salts grafted on cotton fibres for long-term antimicrobial activity. *React. Funct. Polym.* 87, 22-28, and references cited therein.

- 1
2
3
4
5
6
7
8
9
10
11
12
13
14
15
16
17
18
19
20
21
22
23
24
25
26
27
28
29
30
31
32
33
34
35
36
37
38
39
40
41
42
43
44
45
46
47
48
49
50
51
52
53
54
55
56
57
58
59
60
44. Li, T.H., Jing, C. Q., Gao, K. L., Yue, W. Y., Li, S. F. (2015) Cytotoxicity of 1-dodecyl-3-methylimidazolium bromide on HepG2 cells. *Genet. Mol. Res.* 14, 13342-13348.
45. Dobbs, W., Heinrich, B., Bourgogne, C., Donnio, B., Terazzi, E., Bonnet, M. -E., Stock, F., Erbacher, P., Bolcato-Bellemin, A. -L., Douce, L. (2009) Mesomorphic imidazolium salts: new vectors for efficient siRNA transfection. *J. Am. Chem. Soc.* 131, 13338-13346.
46. Adjimani, J. P., Asare, P. (2015) Antioxidant and free radical scavenging activity of iron chelators. *Toxicol. Rep.* 2, 721-728.
47. Darley-Usmar, V. M., Hersey, A., Garland, L. G. (1989) A method for the comparative assessment of antioxidants as peroxy radical scavengers. *Biochem. Pharmacol.* 38, 1465-1469.
48. Puntarulo, S. (2005) Iron, oxidative stress and human health. *Mol Aspects Med.* 26, 299-312.
49. Fleming, R. E., Ponka, P. (2012) Iron overload in human disease. *N Engl J Med.* 366, 348-59.
50. Benedetto, A. (2017) Room-temperature ionic liquids meet bio-membranes: the state-of-the-art. *Biophys Rev.* 9, 309-320.
51. Inoue, M., Wexselblatt, E., Esko, J. D., Tor, Y. (2014) Macromolecular uptake of alkyl chain-modified guanidinoglycoside molecular transporters. *Chembiochem.* 15, 676–680, and the references cited therein.
52. Durand, E., Jacob, R. F., Sherratt, S., Lecomte, J., Baréa, B., Villeneuve, P., Mason, R. P. (2017) The nonlinear effect of alkyl chain length in the membrane interactions of phenolipids: evidence by X-ray diffraction analysis. *Eur. J. Lipid Sci. Technol.* 119, 1600397.

- 1
2
3
4
5
6
7
8
9
10
11
12
13
14
15
16
17
18
19
20
21
22
23
24
25
26
27
28
29
30
31
32
33
34
35
36
37
38
39
40
41
42
43
44
45
46
47
48
49
50
51
52
53
54
55
56
57
58
59
60
53. Conner, S. D., Schmid, S. L. (2003) Regulated portals of entry into the cells. *Nature*, 422, 37-44.
54. Bajbouj, K., Shafarin, J., Hamad, M. (2018) High-dose deferoxamine treatment disrupts intracellular iron homeostasis, reduces growth, and induces apoptosis in metastatic and nonmetastatic breast cancer cell lines. *Technol Cancer Res Treat.* 17, 1-11.
55. Salis, O., Bedir, A., Kilinc, V., Alacam, H., Gulden, S., Okuyucu, A. (2014) The anticancer effects of desferrioxamine on human breast adenocarcinoma and hepatocellular carcinoma cells. *Cancer Biomark.* 14, 419-426.
56. Heath, J. L., Weiss, J. M., Lavau, C. P., Wechsler, D. S. Iron deprivation in cancer-potential therapeutic implications. *Nutrients*5, 2836-2859.
57. Torti, V., Torti, F. M. Iron and cancer: more ore to be mined. *Nat Rev Cancer* 13, 342–355.
58. Tyagi, M., Maity, B., Saha, B., Bauri, A. K., Subramanian, M., Chattopadhyay, S., Patro, B. S.(2018) Spice-derived phenolic, malabaricone B induces mitochondrial damage in lung cancer cells *via* a p53-independent pathway. *Food Funct.* 9, 5715-5727.